



ОБЪЕДИНЕННЫЙ  
ИНСТИТУТ  
ЯДЕРНЫХ  
ИССЛЕДОВАНИЙ  
ДУБНА

E3-94-3

M.A.Ali\*, V.A.Khitrov, Yu.V.Kholnov, O.D.Kjostarova,  
A.M.Sukhovej, A.V.Vojnov, E.V.Vasilieva

THE  $^{196}\text{Pt}$  COMPOUND-STATE  
GAMMA-DECAY CASCADES AFTER THERMAL  
NEUTRON CAPTURE

Submitted to «Zeitschrift für Physik A»

---

\*Present address: Nuclear Physics Department, Atomic Research  
Center, 13759 Cairo, Egypt

1994

Али М.А. и др.

Каскадный гамма-распад компаунд-состояний  $^{196}\text{Pt}$   
после захвата тепловых нейтронов

Экспериментально изучены  $\gamma$ -каскады в  $^{196}\text{Pt}$  после захвата тепловых нейтронов. Изменены интенсивности двухквантовых каскадов, ведущих на три низколежащих уровня этого ядра. В эксперименте идентифицированы все возбужденные состояния  $^{196}\text{Pt}$  до энергии возбуждения около 2,5 МэВ. Определено, что зависимость интенсивности каскадов от энергии первичных переходов принципиально отличается от аналогичной зависимости для распада компаунд-состояний деформированных ядер. Распределение интенсивностей каскадов, заселяющих основное состояние, имеет резонансную форму с центром около 3 МэВ. Этот факт позволяет предположить наличие и влияние на процесс  $\gamma$ -распада компаунд-состояния  $^{196}\text{Pt}$  гигантского магнитного дипольного резонанса.

Работа выполнена в Лаборатории нейтронной физики им. И.М.Франка ОИЯИ.

Препринт Объединенного института ядерных исследований. Дубна, 1994

Ali M.A. et al.

E3-94-3

The  $^{196}\text{Pt}$  Compound-State Gamma-Decay Cascades  
after Thermal Neutron Capture

The  $^{196}\text{Pt}$  compound-state  $\gamma$ -decay cascades following thermal neutron capture were studied in the experiment. The intensities of the two-step cascades leading to the three low-lying levels of this nucleus were measured. All excited states in  $^{196}\text{Pt}$  were identified in the experiment up to the excitation energy of about 2.5 MeV. It was observed that the dependence of the cascades intensity upon the primary transition energy principally differed from that of the transitions following the deformed nuclei compound-state decay. The intensity distribution of the cascades populating the ground-state had a resonance shape with a centroid at about 3 MeV. This fact allows one to assume the presence and the influence of the giant magnetic dipole resonance on the  $^{196}\text{Pt}$  compound-state  $\gamma$ -decay process.

The investigation has been performed at the Frank Laboratory of Neutron Physics, JINR.

# 1 Introduction

An effective method for studying the decay of compound states in nuclei of high level density was developed [1,2] to obtain various information about different nuclei up to an excitation energy approximately equal to the neutron binding energy. Our previous experiments were devoted mainly to deformed nuclei, with most of them lying in the rare-earth element region of the Periodic Table.

For a better understanding of  $\gamma$ -decay modes and to determine their main peculiarities, it is necessary to thoroughly study the different types of nuclei. The data on two-step cascade intensities reveal the peculiarities of the  $\gamma$ -decay process and help determine, at least qualitatively, the factors that influence these decay modes.

The platinum isotopes are situated in a particular region where the stable shape of nuclei changes from a highly deformed (as in the rare-earth nuclei) to a sphere shape (as in *Hg* and *Pb*). For this reason, transitional regions are of special interest for testing nuclear models.

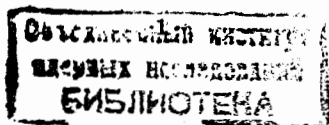
The level scheme of the  $^{196}\text{Pt}$  nucleus was determined either experimentally from the study of the  $^{196}\text{Au}$  and  $^{196}\text{Ir}$  decay [3,4], the stripping (d,p) and the inelastic (d,d') reactions [5,6], the (n, $\gamma$ ) reaction [7,8], and predicted theoretically by the O(6) limit [9], and the IBA model [10]. However, although considerable data have been reported on the low lying levels of the  $^{196}\text{Pt}$  nucleus, our understanding of its structure and decay modes is still unsatisfactory.

The present work is an experimental trial to shed some light on the behaviour of  $\gamma$ -decay cascades in this transitional nucleus and to compare it with the peculiarities of other neighbouring nuclei. So, we analysed two-step cascade intensities from the  $\gamma$ -decay of the compound state after thermal neutron capture and looked for possible GMDR states built on the ground state in this nucleus.

## 2 Experiment

Photon and  $\gamma - \gamma$  coincidence spectra from thermal neutron capture in natural platinum were measured, using the technique of Summed Amplitudes of Coinciding Pulses (SACP). The aim of these measurements was to study the compound state  $\gamma$ -decay of the  $^{196}\text{Pt}$  nucleus. An explicit review of this technique and the method of spectroscopic data analysis can be found in ref. [1,2]. The results of the previous investigations of the intensity distributions of two-step cascades between the compound state and a given low-lying state,  $E_j$ , together with a systematic experimental error analysis were also reported in detail in these works.

The  $\gamma$ -decay transitions of cascades populating the ground and first two excited states in  $^{196}\text{Pt}$  were studied by means of the described method [1,2]. Because of the small partial widths of these types of cascades, and the low efficiency of the Ge(Li) detectors employed, the acquisition time of the experiment was about 400 hours. This was necessary to have meaningful and reasonably precise statistics.



The energy of transitions and the intensity of strong and resolved cascades in the measured spectra (in the form of pairs of peaks) were determined [1] from the two-step cascade intensity distributions. These data are listed in table 1. The energy of the intermediate levels,  $E_M$ , for a certain number of cascades were determined by means of the algorithm [11] which is used for decay schemes construction. This algorithm takes into account the obvious fact that the primary transition in the cascades populating the same intermediate level but different final levels has the same energy and the corresponding peaks of this transition always keep the same position in different measured spectra.

### 3 The $^{196}\text{Pt}$ compound-state $\gamma$ -decay scheme

The principal spectroscopic information about the  $^{196}\text{Pt}$  nucleus was obtained [8] from the studies of thermal and resonance neutron capture and from traditional coincidence investigation methods.

Although this nucleus was the target of many investigations, nevertheless, we have determined for the first time:

- (a) the decay modes for many levels at excitation energies above 2667 keV.
- (b) the new levels at 1880, 1894, 2169 and 2352 keV.

These new levels were populated by  $\gamma$ -transitions from the compound-state decay in  $^{196}\text{Pt}$ . The primary transitions to these states were "masked" by intense transitions to neighbouring levels. In some cases, there was a possibility to identify some intermediate level doublets, *e.g.*, when only a small part of the strong primary transition intensities could be registered [12] in a given spectrum of the intensity distributions. In addition we have used a simple but effective numerical method to improve the energy resolution of the analysed spectra. The bases of this method are given in ref. [13]. Here it should be noted that the presence of doublets at the excitation energies of 1888 and 2170 keV was assumed in the analysis of the primary transition intensities obtained from the capture of neutrons with an average energy of 2 keV [8].

The most important result which can be extracted from the data listed in table 1 is that all the  $0^+$ ,  $1^+$  and  $2^+$  states were revealed experimentally up to an excitation energy not less than 3 MeV. Figure 1 shows a comparison between the observed number of intermediate levels, summed over energy bins of 100 keV, and the calculated values predicted by the model [14].

Note that the observed number of states, for example, at excitation energy below 2.5 MeV considerably exceeds the corresponding numbers predicted by this model. On the other hand, if the parameters  $a$  and  $\delta$  in the model [14] were determined in a way to describe the density of the low-lying excited levels more precisely then the discrepancy between the experimentally measured and the calculated cascade intensities (see below) was even worse.

**Table 1.** A list of energies,  $E_1$  and  $E_2$ , of measured cascade transitions and their relative intensities,  $i_{\gamma\gamma} \pm \Delta i_{\gamma\gamma}$ , in percent of the total intensity of the two-step cascades which have the same total energy.  $E_M \pm \Delta E_M$  is the intermediate level energy.  $E_f$  is the energy of the final state of cascade transitions.

$E_1, \text{keV}$	$E_2, \text{keV}$	$\Delta E_1, \text{keV}$	$i_{\gamma\gamma}$	$\Delta i_{\gamma\gamma}$	$E_M, \text{keV}$	$\Delta E_M, \text{keV}$
$E_1 + E_2 = 7921.0 \text{ keV}$						
6517.0	1404.1	1.25	0.60	0.25	1403.1	0.9
6130.6	1790.5	1.15	0.93	0.32		
6119.1	1802.1	1.61	0.65	0.30	1801.4	0.9
6035.9	1885.2	0.36	3.32	0.41	1886.0	1.2
5952.5	1968.6	0.58	2.11	0.36		
5938.6	1982.5	1.33	0.76	0.32	1983.3	4.3
5752.8	2168.3	1.17	0.75	0.26	2168.8	0.9
5742.2	2178.9	0.88	1.16	0.28		
5734.2	2186.9	1.01	1.02	0.28	2185.1	1.0
5676.3	2244.8	0.54	1.77	0.30	2245.7	2.4
5612.9	2308.2	0.54	2.79	0.45	2308.4	0.8
5549.7	2371.5	1.16	1.25	0.39	2369.9	2.1
5541.4	2379.8	1.37	1.09	0.38	2378.3	1.6
5452.4	2468.7	0.51	3.01	0.46	2468.2	0.8
5309.0	2612.2	0.74	2.25	0.49	2613.3	2.0
5295.9	2625.2	2.06	0.74	0.41		
5241.0	2680.1	1.82	0.82	0.41		
5221.3	2699.8	1.27	1.20	0.43	2702.7	2.9
5187.0	2734.1	0.76	2.81	0.59	2732.4	1.8
5179.8	2741.3	0.70	3.55	0.60	2740.5	1.1
5169.7	2751.4	0.75	2.39	0.51	2753.1	1.5
5099.1	2822.1	1.23	1.31	0.44	2821.7	0.8
5087.7	2833.4	1.90	0.88	0.44	2838.0	3.9
5053.6	2867.5	1.66	1.31	0.52	2864.3	3.1
5046.3	2874.9	0.85	2.57	0.56		
4973.1	2948.0	1.52	1.05	0.43		
4947.7	2973.2	1.40	1.18	0.43		
4904.5	3015.3	1.39	1.40	0.49		
4898.2	3022.9	0.91	2.67	0.55	3021.8	0.8
4882.3	3038.8	1.14	1.54	0.46	3035.8	2.8
4786.1	3134.9	1.37	1.20	0.45		
4741.5	3179.6	1.42	1.21	0.43		
4711.5	3209.6	1.76	1.03	0.44	3210.5	0.9
4661.2	3259.9	1.59	0.98	0.43		

$E_1, \text{keV}$	$E_2, \text{keV}$	$\Delta E_1, \text{keV}$	$i_{\gamma\gamma}$	$\Delta i_{\gamma\gamma}$	$E_M, \text{keV}$	$\Delta E_M, \text{keV}$
4629.4	3291.8	1.95	0.82	0.41	3290.3	1.3
4612.8	3308.4	1.80	0.88	0.41	3309.8	1.8
4470.1	3451.0	1.78	0.89	0.41		
4365.2	3556.0	1.85	0.92	0.44	3554.8	1.2
4265.8	3654.9	1.97	0.80	0.39		
4227.8	3692.0	1.75	0.75	0.34		
4144.3	3776.6	1.83	0.86	0.39		
4107.7	3813.5	1.87	0.83	0.38		
4089.4	3831.5	1.96	0.78	0.35		
4043.6	3875.4	1.72	0.96	0.41		
3890.5	4030.6	1.44	1.08	0.42	4029.1	3.6
$E_1 + E_2 = 7565.0 \text{ keV}$						
6786.6	778.4	1.04	0.62	0.26		
6561.0	1004.0	1.21	0.59	0.26		
6518.5	1046.5	0.64	1.23	0.29	1403.1	0.9
6100.7	1464.3	0.92	1.14	0.35		
6075.9	1488.9	0.76	1.45	0.36		
6040.9	1524.0	1.08	0.99	0.35		
6033.3	1531.7	0.44	2.97	0.44	1886.0	1.2
6004.0	1561.0	0.33	3.72	0.47	1916.9	0.9
5943.4	1621.6	1.35	0.89	0.40	1983.3	4.3
5904.4	1660.6	0.80	1.59	0.42	2014.8	1.9
5854.2	1710.8	1.50	0.80	0.37	2070.9	3.4
5828.0	1737.0	1.05	1.21	0.39	2092.7	0.8
5798.5	1766.5	1.33	0.89	0.39		
5760.3	1804.7	0.67	1.95	0.46	2161.2	0.8
5751.4	1813.6	1.23	1.01	0.39	2168.8	0.9
5737.7	1827.3	1.10	1.12	0.40	2185.1	1.4
5724.3	1840.7	1.18	1.04	0.39	2197.9	1.1
5677.8	1887.2	1.65	0.78	0.38	2245.7	2.4
5612.2	1952.8	0.90	1.88	0.48	2308.4	0.8
5601.1	1964.0	1.19	1.16	0.44		
5453.2	2111.8	1.03	1.50	0.46	2468.2	0.8
5398.4	2166.6	1.30	1.05	0.42	2524.4	1.7
5305.2	2259.8	1.49	0.93	0.42	2613.3	2.0
5261.3	2303.8	0.78	2.66	0.61	2659.0	0.8
5253.2	2311.8	0.52	5.06	0.69	2667.1	0.8
5219.4	2345.6	1.34	1.29	0.48	2702.7	2.9
5198.6	2366.4	1.12	1.53	0.49		

$E_1, \text{keV}$	$E_2, \text{keV}$	$\Delta E_1, \text{keV}$	$i_{\gamma\gamma}$	$\Delta i_{\gamma\gamma}$	$E_M, \text{keV}$	$\Delta E_M, \text{keV}$
5181.9	2383.1	1.54	1.22	0.49	2740.5	1.1
5172.9	2392.1	0.73	4.00	0.71		
5166.2	2398.8	1.41	1.81	0.64	2753.1	1.5
5099.1	2465.9	0.65	3.00	0.57	2821.7	0.8
5078.3	2486.7	1.75	0.94	0.48	2838.0	3.9
5059.8	2505.2	1.05	1.64	0.51	2864.3	3.1
4900.1	2664.9	2.29	0.79	0.45	3021.8	0.8
4888.0	2677.0	2.06	0.83	0.43	3035.8	2.8
4877.7	2687.3	0.82	2.23	0.54	3044.7	2.9
4795.5	2769.5	1.63	1.04	0.47		
4699.5	2865.6	1.93	0.90	0.48		
4631.8	2933.2	1.82	0.88	0.48	3290.3	1.3
4448.8	3116.2	1.57	0.96	0.43	3472.0	1.3
4366.9	3198.1	1.53	0.93	0.47	3554.8	1.2
4180.1	3384.8	2.20	0.82	0.45		
4004.3	3560.7	1.23	1.43	0.48		
3933.3	3631.7	2.13	0.87	0.47		
3924.1	3640.9	1.63	1.27	0.48		
3887.7	3677.3	2.18	0.79	0.44	4029.1	3.6
3787.8	3777.2	1.04	1.93	0.55		
$E_1 + E_2 = 7233.0 \text{ keV}$						
6313.9	919.2	1.20	0.85	0.41		
6119.8	1113.2	1.04	1.03	0.43	1801.4	0.9
6035.6	1197.4	0.74	2.06	0.54	1886.0	1.2
6027.1	1205.9	1.59	0.81	0.46		
6004.4	1228.7	1.63	0.78	0.46	1916.9	0.9
5933.1	1300.0	0.86	1.49	0.50	1983.3	4.3
5908.2	1324.9	1.15	1.06	0.47	2014.8	1.9
5847.8	1385.3	1.11	1.19	0.47	2070.9	3.4
5828.6	1404.4	0.92	1.39	0.49	2092.7	0.8
5759.3	1473.7	1.12	1.80	0.68	2161.2	0.8
5735.6	1497.5	2.17	0.82	0.61	2185.1	1.4
5726.6	1506.4	2.05	1.90	1.18		
5722.1	1510.9	1.10	3.49	1.29	2197.9	1.1
5672.1	1560.9	1.30	1.45	0.63	2245.7	2.4
5576.8	1654.5	1.71	1.17	0.61		
5569.6	1663.0	1.27	1.51	0.60		

$E_1, \text{keV}$	$E_2, \text{keV}$	$\Delta E_1, \text{keV}$	$i_{\gamma\gamma}$	$\Delta i_{\gamma\gamma}$	$E_M, \text{keV}$	$\Delta E_M, \text{keV}$
5553.8	1679.3	1.57	1.14	0.61	2369.9	2.1
5544.5	1688.5	1.57	1.15	0.60	2378.3	1.6
5499.8	1733.3	1.30	1.36	0.60		
5458.3	1774.8	1.36	1.34	0.60		
5424.9	1808.1	1.40	1.34	0.58		
5394.9	1838.1	0.86	2.25	0.66	2524.4	1.7
5262.7	1970.4	0.57	4.87	0.87	2659.0	0.8
5254.6	1978.4	0.27	13.35	1.21	2667.1	0.8
5214.3	2018.7	1.23	1.42	0.59	2702.7	2.9
5190.6	2042.5	1.31	1.50	0.61	2732.4	1.8
5167.2	2065.8	1.08	1.91	0.65	2753.1	1.5
5100.0	2133.1	1.54	1.53	0.72	2821.7	0.8
5083.2	2149.8	1.77	1.35	0.72	2838.0	3.9
5005.7	2227.1	1.74	1.41	0.69		
4899.8	2333.2	1.10	2.35	0.79	3021.8	0.8
4872.5	2360.5	1.87	1.33	0.71	3044.7	2.9
4811.0	2422.0	1.53	1.67	0.73		
4710.1	2522.9	0.91	3.06	0.85	3210.5	0.9
4609.3	2623.8	1.99	1.21	0.71	3309.8	1.8
4596.0	2637.0	1.72	1.42	0.76		
4513.0	2719.6	1.87	1.32	0.66		
4485.7	2747.3	0.91	3.10	0.84		
4449.2	2783.9	1.92	1.39	0.74	3472.0	1.3
4434.0	2799.1	1.61	1.55	0.66		
4373.6	2859.7	1.81	1.24	0.66		
4194.0	3039.1	1.95	1.15	0.58		
4022.7	3210.3	1.73	1.31	0.63		
3896.3	3336.8	1.70	1.34	0.61	4029.1	3.6
3677.5	3555.9	1.63	1.33	0.60		
3637.8	3595.3	1.20	2.03	0.68		

The comparison between the data, as for example in figure 1, with the data of other nuclei shows that for any type of nuclei:

(a) the energy dependence of the level density cannot be described with a simple exponential curve. On the contrary, it has a more complicate character. This statement refers at least to the states populated by intense primary transitions,

(b) the average probability for exciting levels with the same  $J^\pi$  value depends on the level structure, and

(c) the  $(n, \gamma)$  reaction was found to be selective contrary to generally accepted opinion.

#### 4 Averaged intensity of cascades

It is impossible to experimentally determine the sequence of quanta in gamma cascades by means of simple measurements using Ge-detectors. However, from a knowledge of the decay scheme (using the algorithm [11]) and making an accounting as the density of levels increases, and the cascades intensity decreases, with the increase in the excitation energy, it is possible to experimentally decompose the measured intensity distributions into two components corresponding to primary and secondary transition registered events.

Table 1 gives the relative intensities of the measured cascades. The absolute values (in % per capture) could be obtained by normalizing the relative intensities to the absolute intensities [15] of the primary transitions at 5099, 5173, 5612 and 6035 keV using our data for the branching ratios of the corresponding decaying states.

The dependence of the sum intensity of cascades populating the three low-lying levels in  $^{196}\text{Pt}$  upon the energy of the primary transitions is presented in figure 2. The intensities are summed over energy bins of 0.5 MeV. In this figure the experimental data are compared with values calculated in the frame of two different forms of level density models[14,16].

A sharp increase in cascade intensities (with primary transition energies of 5-6 MeV) was observed in this nucleus. This result is in accordance with the previous data obtained from spherical nuclei studies. Practically, there are no enhanced cascades with primary transition energies of about 2-3 MeV.

This latter result leads to the unambiguous conclusion that observed [17-19] enhanced cascades in the  $^{156,158}\text{Gd}$  and  $^{164}\text{Dy}$  nuclei with low-energy primary transitions represent a peculiarity for deformed nuclei (at least, for nuclei that lie at the beginning of the 4s neutron resonance strength function region). The data of  $\gamma$ -decay cascades for spherical nuclei point out that the main peculiarity for these nuclei is the enhancement of primary transition widths at an energy of 5-6 MeV.

In other words, the existing ideas about the constancy of the radiative strength function for the  $\gamma$ -transitions between complex structure states can only be true for the region in which the shell effects do not influence the transitions widths.



**Table 2.** Experimental,  $I_{\gamma\gamma}^{exp}$ , and calculated,  $I_{\gamma\gamma}^{cal}$ , sum intensities of two-step cascades populating a given level  $E_f$  of the  $^{196}\text{Pt}$  nucleus (% per decay)

$E_f$ , keV	$I_{\gamma\gamma}^{exp}$	$I_{\gamma\gamma}^{cal}$ , models	
		[14]	[16]
0	12.2(9)	3.8	4.9
356	9.5(9)	8.2	12.1
668	10.1(21)	5.0	7.6

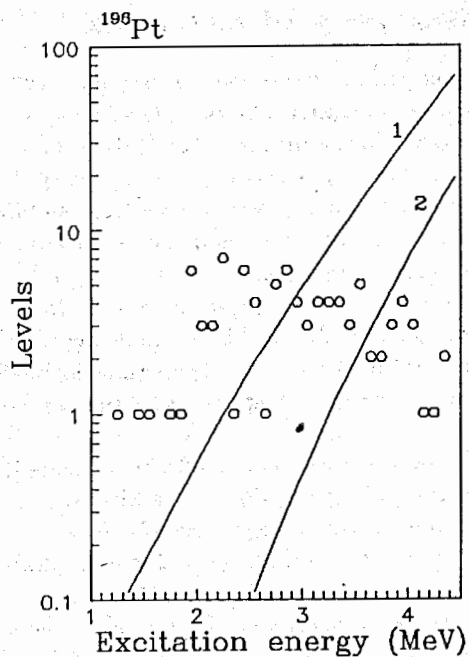


Fig.1. Number of observed levels with  $J^\pi = 0^+, 1^+$  and  $2^+$  in  $^{196}\text{Pt}$  for an excitation energy interval of 100 keV (points). Curves 1 and 2 represent the BSGF (ref.[14]) and the Ignatyuk thermodynamical (ref.[16]) model predictions.

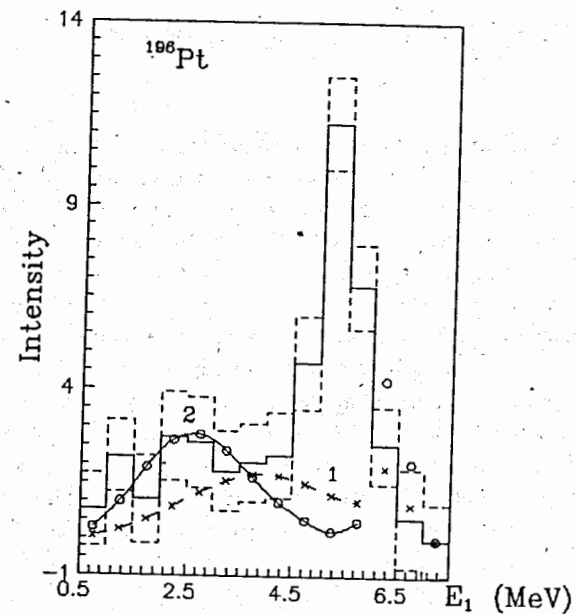


Fig.2. Sum intensity of cascades for the three low-lying levels in  $^{196}\text{Pt}$  (% per decay) as a function of primary transition energy. Histograms represent the experimental data with ordinary statistical errors; curves 1 and 2 correspond to predictions according to the models mentioned in ref.[14,16] respectively.

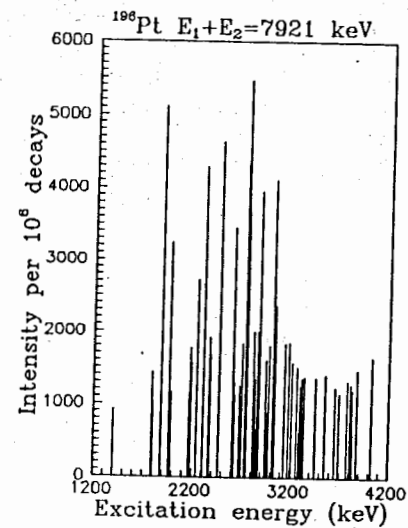


Fig.3. The intensity of two-step cascade transitions of the type  $1^- \rightarrow J^\pi \rightarrow 0^+$  in  $^{196}\text{Pt}$  versus the excitation energy of nucleus.

## 5 The $1^+$ states and possible giant magnetic resonances

As seen in figure 1, all states excited by primary E1-transitions in  $^{196}\text{Pt}$  with spin  $1^+$  were revealed in the experiment up to an excitation energy of about 3 MeV or higher. Some of these states can have a collective structure and the strength of the giant magnetic dipole resonance (GMDR) can be fragmented over these states. If this is true, then the intensity enhancement of the corresponding cascades due to this resonance could be observed experimentally. The  $^{196}\text{Pt}$  compound-state is almost pure, with  $J^\pi=1^-$  [20]. The cascades, with two dipole transitions, populating the  $0^+$  ground-state excite mainly the  $1^+$  intermediate levels and, to a lower extent, the  $1^-$  states. Cascades with quadrupole electric transitions are also possible, but their average intensity is at least ten times less than that for dipole transitions [1].

The intensity dependence of cascades of the type  $1^- \Rightarrow 1^\pm \Rightarrow 0^+$  in  $^{196}\text{Pt}$ , as a function of excitation energy, is demonstrated in figure 3. The figure shows that this dependence has a resonance form with a centroid at  $E_{ex} \simeq 2.8$  MeV, and a width at half maximum of about 1 MeV.

A conclusion about the special character of the excitation and decay of intermediate levels in cascade decay (table 2) can be drawn directly from a comparison of the sums of the cascade absolute intensities for the cascades leading to the three low-lying states in  $^{196}\text{Pt}$ . All listed intensities are similar, and are practically equal. This result disagrees with all the data obtained from even-even nuclei where the ground and first excited states are populated by cascades with dipole transitions. At the same time, both the model calculation and data of, for example, the  $^{156,158}\text{Gd}$  nuclei [16,17] show that the intensity of the cascades leading to the ground-state in  $^{196}\text{Pt}$  should be two times less than those populating the first excited state. This fact points to the special behaviour of the secondary transitions of cascades populating the ground-state of this nucleus.

## 6 Conclusion

The present study leads to the following observations:

1. There is a sharp increase in the intensity of cascades whose primary transition energies are of about 5-6 MeV.
2. It is impossible to predict the density of excited states and intensity of cascades in the frame of any simple nuclear model. This conclusion holds true for all the previously investigated nuclei.
3. Enhanced cascades from the compound-state (neutron resonance) to the ground-state in the  $^{196}\text{Pt}$  nucleus allows one to assume the presence and the influence

of the giant magnetic dipole resonance on the radiative widths of the secondary transitions.

The work has been performed under the auspices of RFFR, grant No. 93-02-16039.

## References

1. Boneva, S.T., Vasilieva, E.V., Popov, Yu.P., Sukhovoij, A.M., Khitrov, V.A.: Sov. J. Part. Nucl. 22(2), 232 (1991)
2. Boneva, S.T., Vasilieva, E.V., Kulik, V.D., Le Hong Khiem, Malov, L.A., Popov, Yu.P., Sukhovoij, A.M., Pham Dinh Khang, Khitrov, V.A., Kholnov, Yu.V., Beitins, M.R., Bondarenko, V.A., Kuvaga, I.L., Prokofiev, P.T., Simonova, L.I., Rezvaya, G.L.: Sov. J. Part. Nucl. 22(6), 698 (1991)
3. Jansen, J.F.W. and Pauw, H.: Nucl. Phys. A94, 235 (1967)
4. Jansen, J.F.W., Pauw, H. and Toest: Nucl. Phys. A115, 321 (1968)
5. Cohen, B.L. and Price, R.E.: Phys. Rev. 118, 1582 (1960)
6. Mukherjee, P.N., Nucl. Phys. 64, 65 (1965)
7. Samour, C., Jackson, H.E., Julien, J., Bloch, A., Lopata, C., Morgenstern, J.: Nucl. Phys. A121, 65 (1968)
8. Cizewski, J.A., Casten, R.F., Smith, G.J., Macphail, M.R., Stelts, M.L., Kane, W.R., Borner, H.G., Davidson W.F.: Nucl. Phys. A323, 349 (1979)
9. Arima, A., Iachello, F.: Phys. Rev. Lett. 40, 385 (1978)
10. Cizewski, J.A., Casten, R.F., Smith, G.J., Stelts, M.L., Kane, W.R., Borner, H.G., Davidson W.F.: Phys. Rev. Lett. 40, 167 (1978)
11. Popov, Yu.P., Sukhovoij, A.M., Khitrov, V.A., Yazvitsky, Yu.S.: Izv. Acad. Nauk SSSR Ser. Fiz. 48, 891 (1984)
12. Beitins, M.R., Boneva, S.T., Khitrov, V.A., Malov, L.A., Popov Yu.P., Prokofiev, P.T., Rezvaya, G.L., Simonova, L.I., Sukhovoij A.M., Vasilieva, E.V.: Z. Phys. A - Hadrons and Nuclei 341, 155 (1992)
13. Sukhovoij, A.M., Khitrov, V.A.: Sov. J. Prib. Tekhn. Eksp. 5, 27 (1984)
14. Dilg, W., Schantl, W., Vonach, H., Uhl, M.: Nucl. Phys. A217, 269 (1973)
15. Lone, M.A., Leavist, R.A., Harrison, D.A.: Nucl. Data Tables 26, 511 (1971)



16. Ignatyuk, A.V., Smirenkin, G.N., Tishin, A.S.: *Yad. Fiz.* 21, 485 (1975)
17. Vasilieva, E.V., Vojnov, A.V., Kestaroova, O.D., Kulik, V.D., Sukhovoij, A.M., Khitrov, V.A., Kholnov, Yu.V., Shilin, V.N.: *Izv. RAN Ser. Fiz.* 57(10), 98 (1993)
18. Ali, M.A., Bogdzal, A.A., Khitrov, V.A., Kholnov, Yu.V., Kulik, V.D., Khiem, L.H., Tuan, N.T., Khang, P.D., Popov, Yu.P., Shilin, V.N., Sukhovoij, A.M., Vasilieva, E.V., Vojnov, A.V.: *JINR preprint E3-91-428* (1991)
19. Vasilieva, E.V., Vojnov, A.V., Kestaroova, O.D., Kulik, V.D., Sukhovoij, A.M., Khitrov, V.A., Kholnov, Yu.V., Shilin, V.N.: *Izv. RAN Ser. Fiz.* 57(10), 109 (1993)
20. Mughabghab, S.F.: *Neutron Cross Sections 1, Part B.* New York: Academic Press 1984

Received by Publishing Department  
on January 5, 1994.